

**Manuscript version: Author's Accepted Manuscript**

The version presented in WRAP is the author's accepted manuscript and may differ from the published version or Version of Record.

**Persistent WRAP URL:**

<http://wrap.warwick.ac.uk/141175>

**How to cite:**

Please refer to published version for the most recent bibliographic citation information. If a published version is known of, the repository item page linked to above, will contain details on accessing it.

**Copyright and reuse:**

The Warwick Research Archive Portal (WRAP) makes this work by researchers of the University of Warwick available open access under the following conditions.

Copyright © and all moral rights to the version of the paper presented here belong to the individual author(s) and/or other copyright owners. To the extent reasonable and practicable the material made available in WRAP has been checked for eligibility before being made available.

Copies of full items can be used for personal research or study, educational, or not-for-profit purposes without prior permission or charge. Provided that the authors, title and full bibliographic details are credited, a hyperlink and/or URL is given for the original metadata page and the content is not changed in any way.

**Publisher's statement:**

Please refer to the repository item page, publisher's statement section, for further information.

For more information, please contact the WRAP Team at: [wrap@warwick.ac.uk](mailto:wrap@warwick.ac.uk).

# Joint Bi-Static Radar and Communications Designs for Intelligent Transportation

Ning Cao, Yunfei Chen, *Senior Member, IEEE*, Xueyun Gu, Wei Feng, *Senior Member, IEEE*

**Abstract**—The cooperation of radar and communications becomes important in vehicular environments due to the demand for radar-assisted communications or communications-assisted radar. In this paper, the tradeoff between bi-static radar and communications in a joint radar-communications setting is studied. We propose three schemes by using time division, superposition or their mixture. For each scheme, three optimization problems are formulated to maximize either the probability of detection for radar subject to a minimum communications rate, the communications rate subject to a minimum probability of detection for radar, or a combined measure of tradeoff. Specifically, given a fixed amount of total time or power for both communications and radar, the optimal power allocation and/or time allocation between radar and communications are derived. Numerical results show that the superposition scheme outperforms the time division scheme and the mixture scheme with considerable performance gains. They also show that the surveillance channel in radar and the communications channel are more important than the direct channel in radar.

**Index Terms**—Bi-static radar, communications, optimization, probability of detection, rate.

## I. INTRODUCTION

Recently, there is an urgent demand for the integration of radar and communications. This is further motivated by emerging applications in intelligent transportation, where the system topology and surroundings are time-variant so that the intelligent vehicles will not only sense the driving environment but also need to exchange information with each other for efficient maneuvers [1] - [3]. For example, in [4], [5], radar signals were sent to determine the channel parameters, based on which vehicle-to-vehicle communications data were exchanged. In [6], vehicles performed collaborative positioning, where features were communicated between vehicles during collaboration. In a densely populated urban environment, joint radar and communications is needed either in the form of radar-assisted vehicular communications [7], where radar sensing provides key system information on the driving environment to improve vehicular communications performance,

The work of Ning Cao was supported in part by the National Natural Science Foundation of China (41830110). The work of Wei Feng was supported in part by the National Natural Science Foundation of China (61941104, 61922049, 61701457, 61771286) and the Beijing Innovation Center for Future Chip. The corresponding author is Wei Feng.

Ning Cao is with the College of Computer and Information, Hohai University, Nanjing, China, 211100. (e-mail: caoning@vip.163.com).

Yunfei Chen and Xueyun Gu are with the School of Engineering, University of Warwick, Coventry, U.K. CV4 7AL (e-mail: Yunfei.Chen@warwick.ac.uk).

Wei Feng is with the Beijing National Research Center for Information Science and Technology, Department of Electronic Engineering, Tsinghua University, Beijing 100084, China, and also with the Peng Cheng Laboratory, Shenzhen 518055, China (e-mail: fengwei@tsinghua.edu.cn).

or in the form of communication-assisted sensing, where communication is used to exchange information between vehicles to improve radar sensing, or simply to reduce the number of devices for fuel-efficiency. This is why the cooperation of radar and communications is important in vehicular networks. In other applications, such as oceans and remote areas, joint radar and communication systems can also be used to detect faraway objects using radar before any communication is performed, due to limited infrastructure. In all these applications, both communications and radar functions are required. These developments call for new investigations into the integration of radar and communications functions. To this end, there have been several areas of investigation.

The first area focuses on the coexistence or cooperation of radar and communications. For example, in [8] and [9], the effects of interference were evaluated. In [10], interference cancellation was considered. These works operate radar and communications in a non-cooperative manner. Radar and communications can also share certain information for cooperation. For instance, [11] - [13] optimized communications and radar subject to constraints from radar and communications, respectively. Another important method is null space projection, where the radar signal was projected onto the null space of the interference channel to avoid interference [14]. Finally, a full cooperation can be incorporated by focusing on the co-design of radar and communications to enable a full cooperation. To achieve the co-design, dual-functional waveform can be used [15] - [18]. Millimeter wave is also promising in such a system [19]. The dual-functional waveform method uses the same waveform for both radar and communications. Since radar and communications have quite different requirements, the tradeoff between radar and communications often leads to complicated waveform designs. This complexity could be reduced by focusing on the tradeoffs of other transmission parameters, such as transmission power and transmission time, as in [20] - [24]. Among them, [20] - [21] focused on the radar function by designing different detectors with or without a reference signal, while [24] studied the tradeoff between radar detection and communications rate in a unified system. However, references [20] - [24] did not provide a comprehensive investigation on such designs.

The aforementioned works have provided very useful guidance on the designs of joint radar and communications systems. These methods have their own advantages and disadvantages. The coexistence or cooperation method requires few changes to existing systems. Hence, it has low implementation cost and is suitable for non-cooperative legacy systems that cannot be changed or state-of-the-art systems that allow few

changes. However, this method incurs mutual interference between radar and communications leading to poor performances. The co-design method is complicated, as radar and communications are integrated in the same system, which requires fundamental changes to existing separate designs and incurs high cost. However, because of the full cooperation, its performance is also the best. This is suitable for new emerging systems. These methods are similar in principle because they all share spectrum between radar and communications. Their main difference is the level of cooperation, with less cooperation for coexistence or cooperation and more cooperation for co-design, leading to different implementation costs and performances. They are also similar to cognitive radios, where coexistence or cooperation are similar to interweave or underlay systems, while co-design is similar to overlay system. However, in cognitive radios, primary users have priorities, while in joint radar-communications both radar and communications have equal status. A more detailed discussion and comparison can be found in survey papers, such as [28]. Due to the length restriction, they are not repeated here.

The research problem tackled in this work is to provide a comprehensive study of joint radar and communications designs extending [20] - [24]. To do this, we split the whole signal into two parts in the time domain using time division, in the power domain using superposition and in a mixed way in both time and power domains. The probability of detection for radar, the information rate for communications, and a defined measure of tradeoff are analyzed. Then, the transmission power and transmission time for radar and communications are optimized. Numerical results are presented to show that the superposition scheme outperforms the time division scheme and the mixture scheme with considerable performance gains. This is because the superposition scheme has larger signal amplitude and longer information transmission time so that the radar detector has higher probability of detection and the communications receiver has larger rate. They also show the effects of different system parameters on the performance tradeoff.

The novelty and the main contributions of this work can be summarized as follows:

- Compared with [20] - [24], our work focuses on both radar and communications, while [20] - [24] mainly focused on radar. Also, our work proposes three different schemes each with three different optimization problems based on detailed analysis, while [20] - [24] considered simple optimization with little analysis.
- The power and/or time allocation between radar and communications for each proposed scheme is optimized. The derived optimal values are either solved in closed-form or determined by a single-variable equation.
- The performance of the unified radar-communications system is examined for different system parameters to provide design guidance.

## II. SYSTEM MODEL

Consider a joint radar and communications system with one radar/communications transmitter, one target, one radar

TABLE I  
LIST OF FREQUENTLY USED SYMBOLS

Symbol	Definition
$C$	Information rate for communications
$DP$	Probability of detection
$FA$	Probability of false alarm
$h_c$	Channel coefficient from transmitter to communications receiver
$h_d$	Direct channel coefficient from transmitter to radar receiver
$h_s$	Surveillance channel coefficient from transmitter to radar receiver
$K$	Number of samples for communications
$L$	Number of samples for radar
$N$	Total number of samples
$P_c$	Transmission power for communications
$P_r$	Transmission power for radar
$P_T$	Total transmission power
$T$	Total transmission time
$T_c$	Transmission time for communications
$T_r$	Transmission time for radar
$T_s$	Sampling interval
$U$	Measure of tradeoff
$w_{ci}$	The $i$ -th sample of communications signal
$w_{ri}$	The $i$ -th sample of radar signals
$\sigma^2$	Noise power
$\gamma_c$	Signal-to-noise ratio of communications
$\lambda$	Detection threshold for radar
$\alpha$	Power allocation coefficient
$\beta$	Time allocation coefficient
$\epsilon$	Tradeoff coefficient
$\gamma_d$	Signal-to-noise ratio in direct channel
$\gamma_s$	Signal-to-noise ratio in surveillance channel

receiver and one communications receiver, as shown in Fig. 1. The target to be detected could be nearby vehicles or pedestrians. The transmitter is a base station whose signal is used for both communications and radar but not as target. For simplicity, each node has a single antenna. Multiple antennas may also be used to increase achievable rate for communications and improve detection performance for radar but are not discussed in this work [25], [26]. The radar function is performed in a bi-static and omnidirectional configuration, where the signal travels from the transmitter to the radar receiver in the direct channel as a reference signal, as well as reflected by the target in the surveillance channel, if the target exists. Existing target detectors at autonomous vehicles often use active mono-static sensors including radar, LiDAR and cameras. These sensors can be fused with the passive bi-static radar studied here for better performance [27]. Also, radar normally uses omnidirectional setting to detect target, as in this work, before it uses directional setting to track target. The communications function is performed in a conventional point-to-point configuration, where the information is sent from the transmitter to the communications receiver directly. The transmitter is stationary and its location is known in the system. The model in Fig. 1 is similar to that in [20] - [24]. A list of frequently used symbols is given in Table I.

Without loss of generality, assume that the total transmission time is  $T$  seconds and the total transmission power is  $P_T$  for both radar and communications. Also, assume that the transmission time, the transmission power for radar and the transmission time, the transmission power for communications are  $T_r$ ,  $P_r$  and  $T_c$ ,  $P_c$ , respectively. Denote  $T_s$  as the sampling interval. Also, block fading channel is assumed so that the

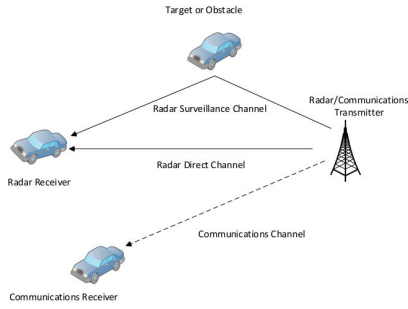


Fig. 1. Diagram of the considered joint passive radar and communications system.

channel coefficients do not change within  $T$  seconds.

#### A. Time division

For the time-division scheme, the signal is split in the time domain into two parts. Hence, one has  $T_c + T_r = T$  and  $P_c = P_r = P_T$ . Specifically, the received signal at the communications receiver is given by

$$y_{ci} = \sqrt{P_T} h_c w_{ci} + n_{ci} \quad (1)$$

where  $i = 1, 2, \dots, K$  is the sample index,  $K = \frac{T_c}{T_s}$  is the total number of samples for communications,  $T_c$  is the time duration for communications as defined before,  $h_c$  is the complex channel coefficient from the transmitter to the communications receiver,  $w_{ci}$  is the transmitted signal, and  $n_{ci}$  is the complex additive white Gaussian noise (AWGN) with mean zero and variance  $\sigma^2$ . Assume constant modulus modulation schemes in our work so that the transmitted signal satisfies  $|w_{ci}|^2 = 1$ . For example, this is the case when phase shift keying (PSK) is used. The PSK modulation is widely used in communications systems.

These  $K$  samples can be stacked into a vector as

$$\mathbf{y}_c = \sqrt{P_T} h_c \mathbf{w}_c + \mathbf{n}_c \quad (2)$$

where  $\mathbf{y}_c = [y_{c1}, y_{c2}, \dots, y_{cK}]^T$ ,  $\mathbf{w}_c = [w_{c1}, w_{c2}, \dots, w_{cK}]^T$  and  $\mathbf{n}_c = [n_{c1}, n_{c2}, \dots, n_{cK}]^T$  are all  $K \times 1$  vectors and  $[\cdot]^T$  represents the transpose operation. In (2), it is assumed that the noise samples are independent of each other so that the covariance matrix of  $\mathbf{n}_c$  is given by  $\sigma^2 \mathbf{I}_K$ , where  $\mathbf{I}_K$  is the  $K$ -th order identity matrix.

Using the signal in (1), the information rate for communications can be derived as

$$C = T_c \log_2(1 + P_T \gamma_c) \quad (3)$$

where  $\gamma_c = \frac{|h_c|^2}{\sigma^2}$  is the signal-to-noise (SNR) ratio of the communications channel. It is known from communications theories that (3) requires Gaussian inputs. Otherwise, it is only an upper limit representing achievable rate. This includes the case when non-Gaussian radar interference occurs. In this case, (3) is still a very useful measure of rate that has been widely used in wireless communications.

The other part of the signal is used for radar. Specifically, the radar detection problem can be formulated as a binary hypothesis testing problem as [20] - [24]

$$H_0 : \begin{cases} y_{di} = \sqrt{P_T} h_d w_{ri} + n_{di} \\ y_{si} = n_{si} \end{cases} \quad (4)$$

for the null hypothesis and

$$H_1 : \begin{cases} y_{di} = \sqrt{P_T} h_d w_{ri} + n_{di} \\ y_{si} = \sqrt{P_T} h_s w_{ri} + n_{si} \end{cases} \quad (5)$$

for the alternative hypothesis, where  $i = 1, 2, \dots, L$  is the sample index,  $L = \frac{T_r}{T_s}$ ,  $T_r$  is the time duration for sensing as defined before,  $h_d$  is the complex channel coefficient from the transmitter to the radar receiver in the direct channel,  $h_s$  is the complex channel coefficient from the transmitter to the radar receiver via the target in the surveillance channel,  $w_{ci}$  is the transmitted signal for radar detection,  $n_{di}$  and  $n_{si}$  are the complex AWGN with mean zero and variance  $\sigma^2$ . We have used the same signal model in (4) and (5), as in [20] - [24] that ignore Doppler, angle or resolution detection. Detailed discussion can be found in [20] - [24].

By stacking the samples into vectors, one further has

$$H_0 : \begin{cases} \mathbf{y}_d = \sqrt{P_T} h_d \mathbf{w}_r + \mathbf{n}_d \\ \mathbf{y}_s = \mathbf{n}_s \end{cases} \quad (6)$$

for the null hypothesis and

$$H_1 : \begin{cases} \mathbf{y}_d = \sqrt{P_T} h_d \mathbf{w}_r + \mathbf{n}_d \\ \mathbf{y}_s = \sqrt{P_T} h_s \mathbf{w}_r + \mathbf{n}_s \end{cases} \quad (7)$$

for the alternative hypothesis, where  $\mathbf{y}_d$ ,  $\mathbf{y}_s$ ,  $\mathbf{w}_r$ ,  $\mathbf{n}_d$  and  $\mathbf{n}_s$  are all  $L \times 1$  vectors. Similarly, let  $|w_{ri}|^2 = 1$  with constant modulus so that  $\mathbf{w}_r^H \mathbf{w}_r = L$ , where  $(\cdot)^H$  is the Hermitian operation. This is for example the case when linear frequency modulation is used. Again, we assume that the noise samples are independent such that the covariance matrices of  $\mathbf{n}_d$  and  $\mathbf{n}_s$  are both given by  $\sigma^2 \mathbf{I}_L$ . It is also assumed that clutters have already been dealt with so that there is only noise in (6) and (7), the same as that in [20] - [24]. Interested readers are referred to these works for more details.

Note that  $\mathbf{w}_r$  and  $\mathbf{w}_c$  can be different temporal parts of the same signal for communications. It has been reported in [30], [31] and other works that communications signals can be used for target detection in passive radar. They can also be different waveforms multiplexed in time, where  $\mathbf{w}_r$  is a conventional radar waveform while  $\mathbf{w}_c$  is a conventional communications waveform. Our model in (1) - (7) is general enough to include both cases. Note also that, in our work, both  $\mathbf{w}_c$  and  $\mathbf{w}_r$  are assumed unknown but deterministic. The coefficients of the radar channels  $h_d$  and  $h_s$  are not known either.

For unknown signals and unknown channels, the received signals in (6) and (7) can be applied to a generalized likelihood ratio test (GLRT) detector. Details can be found in [20]. Using this detector, the probability of false alarm can be shown as

[24]

$$\begin{aligned}
 FA &= e^{-\lambda} + \frac{2\lambda e^{-(\lambda+P_T L \gamma_d)}}{2^L \Gamma(L)} \sum_{k=0}^{L-2} \sum_{p=0}^k \binom{k}{p} 2^{L-1} \lambda^{k-p} \\
 &\quad \Gamma(L+p-k-1) {}_1F_1(L+p-k-1; L; P_T L \gamma_d) \\
 &\quad - \sum_{k=0}^{L-2} \sum_{p=0}^k \sum_{l=0}^k \frac{\binom{k}{p}}{l!} 2^{k-p-l} \lambda^{k-p} \Gamma(L+l+p-k-1) \\
 &\quad {}_1F_1(L+l+p-k-1; L; 0.5 P_T L \gamma_d) \quad (8)
 \end{aligned}$$

where  $\lambda$  is the detection threshold used in the GLRT detector,  $\gamma_d = \frac{|h_d|^2}{\sigma^2}$  is the SNR of the reference channel from the transmitter to the radar receiver directly,  $\Gamma(\cdot)$  is the Gamma function, and  ${}_1F_1(\cdot; \cdot; \cdot)$  is the hypergeometric function [32]. A closed-form expression for the probability of detection is not available.

When the SNR of the reference channel is very large such that  $\gamma_d \gg 1$ , the probability of false alarm can be approximated as

$$FA \approx e^{-\lambda} \quad (9)$$

and the probability of detection can be approximated as

$$DP \approx Q_1(\sqrt{2P_T L \gamma_s}, \sqrt{2\lambda}) = Q_1(\sqrt{2P_T L \gamma_s}, b) \quad (10)$$

where  $\gamma_s = \frac{|h_s|^2}{\sigma^2}$  is the SNR of the surveillance channel from the transmitter to the radar receiver via the target,  $b = \sqrt{2\lambda} = \sqrt{-2 \ln(FA)}$  is a constant from (9) and  $Q_1(\cdot, \cdot)$  is the first-order Marcum Q function [32]. Note that, since  $T = T_c + T_r$ , one has  $N = K + L$ , where  $N = \frac{T}{T_s}$ .

### B. Superposition

In the superposition scheme, the radar signal and the communications signal are transmitted at the same time over the same frequency. Thus, the received signal at the communications receiver becomes

$$y_{ci} = (\sqrt{P_c} s_{ci} + \sqrt{P_r} s_{ri}) h_c + n_{ci} \quad (11)$$

where  $s_{ci}$  is the transmitted signal for communications,  $s_{ri}$  is the transmitted signal for radar,  $i = 1, 2, \dots, N$  with  $N = \frac{T}{T_s} = K + L$ , and other symbols are defined as before. Again,  $|s_{ci}|^2 = |s_{ri}|^2 = 1$ . In the vector form, the received signal at the communications receiver can be written as

$$\mathbf{y}_c = (\sqrt{P_c} \mathbf{s}_c + \sqrt{P_r} \mathbf{s}_r) h_c + \mathbf{n}_c. \quad (12)$$

The vectors in (12) are  $N \times 1$  vectors.

From (11), the information rate for communications is

$$C = T \log_2 \left( 1 + \frac{P_c \gamma_c}{P_r \gamma_c + 1} \right). \quad (13)$$

Compared with the rate of the time-division scheme in (3), this rate has a larger time duration of  $T$  but a smaller signal-to-interference-plus-noise ratio (SINR) of  $\frac{P_c \gamma_c}{P_r \gamma_c + 1}$ . The rate can be improved by removing the inference from the radar, if the radar waveform is known and subtracted from the received signal in (11). The coefficient of the communications channel can also be estimated in the presence of interference [29]. However, both topics are beyond the scope of the current

work. We assume that the radar interference is random at the communications receiver due to random phase shift so that it cannot be removed.

For radar detection, the binary hypothesis test becomes

$$H_0 : \begin{cases} y_{di} = (\sqrt{P_c} s_{ci} + \sqrt{P_r} s_{ri}) h_d + n_{di} \\ y_{si} = n_{si} \end{cases} \quad (14)$$

$$H_1 : \begin{cases} y_{di} = (\sqrt{P_c} s_{ci} + \sqrt{P_r} s_{ri}) h_d + n_{di} \\ y_{si} = (\sqrt{P_c} s_{ci} + \sqrt{P_r} s_{ri}) h_s + n_{si} \end{cases} \quad (15)$$

where the transmitted signal is  $(\sqrt{P_c} s_{ci} + \sqrt{P_r} s_{ri})$  in this scheme and  $i = 1, 2, \dots, N$ . The vector forms become

$$H_0 : \begin{cases} \mathbf{y}_d = (\sqrt{P_c} \mathbf{s}_c + \sqrt{P_r} \mathbf{s}_r) h_d + \mathbf{n}_d \\ \mathbf{y}_s = \mathbf{n}_s \end{cases} \quad (16)$$

$$H_1 : \begin{cases} \mathbf{y}_d = (\sqrt{P_c} \mathbf{s}_c + \sqrt{P_r} \mathbf{s}_r) h_d + \mathbf{n}_d \\ \mathbf{y}_s = (\sqrt{P_c} \mathbf{s}_c + \sqrt{P_r} \mathbf{s}_r) h_s + \mathbf{n}_s \end{cases} \quad (17)$$

where all vectors are  $N \times 1$  vectors. One sees from (11) - (17) that the radar waveform  $\mathbf{s}_r$  and the communications waveform  $\mathbf{s}_c$  can also be different in the superposition scheme. They can use their respective conventional waveforms. This greatly simplifies the design, compared with the dual-function waveform method in [15]. In (12) and (17), if  $P_c = 0$ , the system becomes a pure radar system, and if  $P_r = 0$ , it becomes a pure communications system. One also sees that the detection in (16) and (17) does not differentiate the radar signal from the communications signal, as they are combined in the signal part of the sample. Thus, the overall signal is used for detection. This brings performance gain to superposition, as will be shown later.

Using (16) and following the same procedures as those used to derive (8), one has the probability of false alarm in the superposition scheme as

$$\begin{aligned}
 FA &= e^{-\lambda} + \frac{2\lambda e^{-(\lambda+W\gamma_d)}}{2^N \Gamma(N)} \sum_{k=0}^{N-2} \sum_{p=0}^k \binom{k}{p} 2^{N-1} \lambda^{k-p} \\
 &\quad \Gamma(N+p-k-1) {}_1F_1(N+p-k-1; N; W\gamma_d) \\
 &\quad - \sum_{k=0}^{N-2} \sum_{p=0}^k \sum_{l=0}^k \frac{\binom{k}{p}}{l! 2^{p+l-k}} \Gamma(N+l+p-k-1) \\
 &\quad {}_1F_1(N+l+p-k-1; N; 0.5W\gamma_d) \quad (18)
 \end{aligned}$$

where  $W = (\sqrt{P_c} \mathbf{s}_c + \sqrt{P_r} \mathbf{s}_r)^H (\sqrt{P_c} \mathbf{s}_c + \sqrt{P_r} \mathbf{s}_r)$ .

Similarly, when the SNR of the direct channel is very large,  $\gamma_d \gg 1$ . In this case, the probability of false alarm can be approximated as

$$FA \approx e^{-\lambda} \quad (19)$$

and the probability of detection can be approximated as

$$DP \approx Q_1(\sqrt{2\gamma_s W}, b). \quad (20)$$

### C. Mixture

In the mixture scheme, the signal is split in both the time domain and the power domain. Hence, in this scheme, the received signal at the communications receiver is given by

$$y_{ci} = \sqrt{P_c} h_c w_{ci} + n_{ci} \quad (21)$$

where  $i = 1, 2, \dots, K$  is the sample index. All the symbols are defined as before, except that  $P_T$  in (1) has been replaced by  $P_c$  in (21). These  $K$  samples are stacked into vectors as

$$\mathbf{y}_c = \sqrt{P_c} h_c \mathbf{w}_c + \mathbf{n}_c. \quad (22)$$

Using the signal in (21), the information rate in this case is derived as

$$C = T_c \log_2(1 + P_c \gamma_c) \quad (23)$$

with  $P_T$  in (3) being replaced by  $P_c$ .

The other part of the signal is used for radar. Specifically, one has

$$H_0 : \begin{cases} \mathbf{y}_d = \sqrt{P_r} h_d \mathbf{w}_r + \mathbf{n}_d \\ \mathbf{y}_s = \mathbf{n}_s \end{cases} \quad (24)$$

for the null hypothesis and

$$H_1 : \begin{cases} \mathbf{y}_d = \sqrt{P_r} h_d \mathbf{w}_r + \mathbf{n}_d \\ \mathbf{y}_s = \sqrt{P_r} h_s \mathbf{w}_r + \mathbf{n}_s \end{cases} \quad (25)$$

where all vectors are  $L \times 1$ . For unknown signals and unknown channels, using the GLRT detector, the probability of false alarm can be shown as

$$\begin{aligned} FA &= e^{-\lambda} + \frac{2\lambda e^{-(\lambda + P_r L \gamma_d)}}{2^L \Gamma(L)} \sum_{k=0}^{L-2} \sum_{p=0}^k \binom{k}{p} 2^{L-1} \lambda^{k-p} \\ &\quad \Gamma(L + p - k - 1) {}_1F_1(L + p - k - 1; L; P_r L \gamma_d) \\ &\quad - \sum_{k=0}^{L-2} \sum_{p=0}^k \sum_{l=0}^k \frac{\binom{k}{p}}{l!} 2^{k-p-l} \lambda^{k-p} \Gamma(L + l + p - k - 1) \\ &\quad {}_1F_1(L + l + p - k - 1; L; 0.5 P_r L \gamma_d). \end{aligned} \quad (26)$$

When the SNR of the reference channel is very large such that  $\gamma_d \gg 1$ , the probability of false alarm can also be approximated as

$$FA \approx e^{-\lambda} \quad (27)$$

and the probability of detection can be approximated as

$$DP \approx Q_1(\sqrt{2P_r L \gamma_s}, \sqrt{2\lambda}) = Q_1(\sqrt{2P_r L \gamma_s}, b). \quad (28)$$

In the next section, we will use these information rates and probabilities of detection to formulate the optimization problems.

### III. PERFORMANCE TRADEOFF AND OPTIMIZATION

Before we formulate the optimization problems, we define two coefficients. Let  $\alpha = \frac{P_r}{P_T}$  be the power allocation coefficient. Thus,  $P_r = \alpha P_T$  and  $P_c = (1 - \alpha) P_T$ , with  $0 \leq \alpha \leq 1$ . Also, define  $\beta = \frac{T_r}{T}$  as the time allocation coefficient. Thus,  $T_r = \beta T$  and  $T_c = (1 - \beta) T$ , which give  $L = \beta N$  and  $K = (1 - \beta) N$ .

Using  $\beta$ , the information rate and the probability of detection in the time-division scheme can be rewritten as

$$C = (1 - \beta) T \log_2(1 + P_T \gamma_c) \quad (29)$$

and

$$DP \approx Q_1(\sqrt{2\beta P_T \gamma_s N}, b) \quad (30)$$

respectively. Similarly, using  $\alpha$ , the information rate and the probability of detection in the superposition scheme can be rewritten as

$$C = T \log_2 \left( 1 + \frac{(1 - \alpha) P_T \gamma_c}{\alpha P_T \gamma_c + 1} \right) \quad (31)$$

and

$$DP \approx Q_1(\sqrt{2\gamma_s P_T N (1 + 2\sqrt{\alpha(1 - \alpha)}\rho)}, b) \quad (32)$$

respectively, where  $\rho = \frac{\mathbf{s}_r^H \mathbf{s}_c + \mathbf{s}_c^H \mathbf{s}_r}{2N}$  gives the correlation coefficient of the radar waveform  $\mathbf{s}_r$  and the communications waveform  $\mathbf{s}_c$ , and using  $\alpha$  and  $\beta$ , the information rate and the probability of detection in the mixture scheme can be rewritten as

$$C = (1 - \beta) T \log_2(1 + (1 - \alpha) P_T \gamma_c) \quad (33)$$

and

$$DP \approx Q_1(\sqrt{2\alpha\beta P_T \gamma_s N}, b) \quad (34)$$

respectively. Next, we will find the values of  $\alpha$  and  $\beta$  that optimize the power and time allocation.

#### A. Time-division

The first optimization problem for time-division is formulated as

$$P_1 : \max_{\beta} \{DP\}, \quad s.t. \quad (35)$$

$$C \geq C_m, \quad (36)$$

$$0 \leq \beta \leq 1 \quad (37)$$

where  $DP$  is given by (30) and  $C$  is given by (29). This optimization is for applications where the radar function is more important than the communications function such that the probability of detection should be maximized subject to a minimum rate.

The second optimization problem for time-division is given by

$$P_2 : \max_{\beta} \{C\}, \quad s.t. \quad (38)$$

$$DP \geq P_m, \quad (39)$$

$$0 \leq \beta \leq 1 \quad (40)$$

where the information rate is maximized subject to a minimum probability of detection. This optimization is for applications where the communications function is more important than the radar function.

In the general case when radar and communications are equally important or when there are no constraints on them, the third optimization problem is given as

$$P_3 : \max_{\beta} \{U\}, \quad s.t. \quad (41)$$

$$0 \leq \beta \leq 1 \quad (42)$$

where  $U$  is the measure of tradeoff defined as

$$U = \epsilon DP + (1 - \epsilon) \frac{C}{C_{max}}, \quad (43)$$

$0 < \epsilon < 1$  is the tradeoff coefficient so that when  $\epsilon > 0.5$ , radar is more important, when  $\epsilon < 0.5$ , communication is

more important, and when  $\epsilon = 0.5$ , they are equally important. In (43),  $C_{max} = T \log_2(1 + P_T \gamma_c)$  is used to normalize the information rate so that both the probability of detection and the normalized information rate are between 0 and 1 for optimization. Next, we solve these optimization problems.

For  $P_1$  in (35), using (29) in (36), one has

$$(1 - \beta)T \log_2(1 + P_T \gamma_c) \geq C_m. \quad (44)$$

Using (44) and (37), one has

$$0 \leq \beta \leq 1 - \frac{C_m}{T \log_2(1 + P_T \gamma_c)} \quad (45)$$

where  $C_m \leq T \log_2(1 + P_T \gamma_c)$  must be satisfied. One sees from (30) that  $DP$  is a monotonic function of  $\beta$  so that the maximum  $DP$  is achieved when  $\beta$  is the largest. Thus, from (45),  $DP$  is maximized when  $\beta = 1 - \frac{C_m}{T \log_2(1 + P_T \gamma_c)}$ . The optimum value of  $\beta$  is

$$\beta_{opt} = \begin{cases} 1 - \frac{C_m}{T \log_2(1 + P_T \gamma_c)}, & C_m \leq T \log_2(1 + P_T \gamma_c) \\ \text{none}, & C_m > T \log_2(1 + P_T \gamma_c) \end{cases} \quad (46)$$

and the maximum  $DP$  is

$$DP^{max} = Q_1(\sqrt{2\beta_{opt} P_T \gamma_s N}, b). \quad (47)$$

For  $P_2$  in (38), using (30) in (39), one has

$$Q_1(\sqrt{2\beta P_T \gamma_s N}, b) \geq P_m. \quad (48)$$

Since the Marcum Q function is monotonic, from (48) one has

$$1 \geq \beta \geq \frac{[Q_1^{-1}(P_m, b)]^2}{2P_T \gamma_s N} \quad (49)$$

where  $Q_1^{-1}(\cdot, \cdot)$  is the inverse function of  $Q_1(\cdot, \cdot)$ . In this case,  $2P_T \gamma_s N \geq [Q_1^{-1}(P_m, b)]^2$  must be satisfied. From (29), the information rate  $R$  increases monotonically as  $\beta$  decreases. Thus, the maximum  $R$  is achieved when  $\beta$  is the smallest. From (49), this is given by  $\beta = \frac{[Q_1^{-1}(P_m, b)]^2}{2P_T \gamma_s N}$ . Then, the optimum  $\beta$  and  $R$  are given by

$$\beta_{opt} = \begin{cases} \frac{[Q_1^{-1}(P_m, b)]^2}{2P_T \gamma_s N}, & 2P_T \gamma_s N \geq [Q_1^{-1}(P_m, b)]^2 \\ \text{none}, & 2P_T \gamma_s N < [Q_1^{-1}(P_m, b)]^2 \end{cases} \quad (50)$$

and

$$C^{max} = (1 - \beta_{opt})T \log_2(1 + P_T \gamma_c) \quad (51)$$

respectively.

For  $P_3$  in (41), there are no constraints on the probability of detection or the information rate so that we can simply take the first-order derivative of  $P_t$  with respect to  $\beta$  and setting it to zero to give

$$\epsilon \frac{\sqrt{P_T \gamma_s N}}{\sqrt{2\beta}} \frac{\partial Q_1(a, b)}{\partial a} = (1 - \epsilon) \quad (52)$$

where  $a = \sqrt{2\beta P_T \gamma_s N}$ . Also, one has  $\frac{\partial Q_1(a, b)}{\partial a} = a[Q_2(a, b) - Q_1(a, b)]$ . Using this relationship in (52), one has

$$\begin{aligned} \frac{1 - \epsilon}{\epsilon P_T \gamma_s N} &= Q_2(\sqrt{2\beta_{opt} P_T \gamma_s N}, b) \\ &- Q_1(\sqrt{2\beta_{opt} P_T \gamma_s N}, b) \end{aligned} \quad (53)$$

which can be used to determine the optimum value for  $\beta$ . The solution to this equation can be found numerically. Then, the optimum  $U$  is calculated as

$$\begin{aligned} U^{max} &= \epsilon Q_1(\sqrt{2\beta_{opt} P_T \gamma_s N}, b) \\ &+ (1 - \epsilon)(1 - \beta_{opt}). \end{aligned} \quad (54)$$

## B. Superposition

For the superposition scheme, similarly, the optimization problems can be formulated as

$$P_4 : \max_{\alpha} \{DP\}, \quad s.t. \quad (55)$$

$$C \geq C_m, \quad (56)$$

$$0 \leq \alpha \leq 1 \quad (57)$$

for applications that maximize the probability of detection subject to a minimum rate, or

$$P_5 : \max_{\alpha} \{C\}, \quad s.t. \quad (58)$$

$$DP \geq P_m, \quad (59)$$

$$0 \leq \alpha \leq 1 \quad (60)$$

for applications that maximize the information rate subject to a minimum probability of detection, or

$$P_6 : \max_{\alpha} \{U\}, \quad s.t. \quad (61)$$

$$0 \leq \alpha \leq 1 \quad (62)$$

in the general case, where  $DP$  is given by (32),  $C$  is given by (31), and other symbols are defined as before. These optimization problems can be solved in the following.

For  $P_4$ , using (31) in (56) and solving the inequality, one has

$$0 \leq \alpha \leq \left(1 + \frac{1}{P_T \gamma_c}\right) 2^{-\frac{C_m}{T}} - \frac{1}{P_T \gamma_c} \quad (63)$$

which again requires that  $C_m \leq T \log_2(1 + P_T \gamma_c)$  when choosing the limiting rate. From (32), one sees that  $DP$  depends on  $\alpha$  through  $\alpha(1 - \alpha)$ , which has the maximum value of  $\frac{1}{4}$  at  $\alpha = \frac{1}{2}$ . Thus, the maximization of  $DP$  is equivalent to the maximization of  $\alpha(1 - \alpha)$ , with respect to  $\alpha$ . This gives the optimum value of  $\alpha$  as

$$\alpha_{opt} = \begin{cases} \frac{1}{2}, & \rho > 0, \frac{\frac{1}{2} + \frac{1}{P_T \gamma_c}}{1 + \frac{1}{P_T \gamma_c}} 2^{\frac{C_m}{T}} < 1 \\ \frac{1 + \frac{1}{P_T \gamma_c}}{2^{\frac{C_m}{T}}} - \frac{1}{P_T \gamma_c}, & \rho > 0, \frac{\frac{1}{2} + \frac{1}{P_T \gamma_c}}{1 + \frac{1}{P_T \gamma_c}} 2^{\frac{C_m}{T}} > 1 \\ 0, & \rho < 0 \end{cases} \quad (64)$$

and the maximum probability of detection as

$$DP^{max} = Q_1(\sqrt{2\gamma_s P_T N (1 + 2\sqrt{\alpha_{opt}(1 - \alpha_{opt})\rho}), b}). \quad (65)$$

For  $P_5$ , it can be seen from (31) that  $C$  monotonically increases when  $\alpha$  decreases. Thus, the maximum  $C$  is achieved at the minimum  $\alpha$  allowed. Using (32) in (59), one has the inequality

$$2\rho\sqrt{\alpha(1 - \alpha)} \geq d - 1 \quad (66)$$

where  $d = \frac{[Q_1^{-1}(P_m, b)]^2}{2P_T\gamma_s N}$ . From (66), the optimum value of  $\alpha$  can be derived as

$$\alpha_{opt} = \begin{cases} 0, & d < 1 \\ \frac{1}{2} - \frac{1}{2}\sqrt{1 - \frac{1}{\rho^2}[d-1]^2} & 1 < d < 1 + \rho \\ \text{none}, & 1 + \rho < d \end{cases} \quad (67)$$

for  $\rho > 0$  and

$$\alpha_{opt} = \begin{cases} 0, & d < 1 + \rho \\ \frac{1}{2} - \frac{1}{2}\sqrt{1 - \frac{1}{\rho^2}[d-1]^2} & 1 + \rho < d < 1 \\ \text{none}, & 1 < d \end{cases} \quad (68)$$

for  $\rho < 0$ . The maximum rate can then be calculated by using  $\alpha_{opt}$  in (31).

For  $P_6$ , by taking the first-order derivative of  $U$  with respect to  $\alpha$  and setting the derivative to zero, one has

$$\begin{aligned} & \frac{(1-\epsilon)\gamma_c}{\epsilon\gamma_s N \rho \log(1+P_T\gamma_c)} \cdot \frac{\sqrt{\alpha_{opt}(1-\alpha_{opt})}}{(1-2\alpha_{opt})(P_T\gamma_c\alpha_{opt}+1)} \\ &= Q_2(\sqrt{2\gamma_s P_T N(1+2\rho\sqrt{\alpha_{opt}(1-\alpha_{opt})}), b}) \\ & - Q_1(\sqrt{2\gamma_s P_T N(1+2\rho\sqrt{\alpha_{opt}(1-\alpha_{opt})}), b}) \end{aligned} \quad (69)$$

that determines the optimum value of  $\alpha$ . This is again a one-variable nonlinear equation that can be numerically solved using common mathematical software, such as MATLAB and Mathematica.

### C. Mixture

Similarly, the first optimization problem for mixture is formulated as

$$P_7 : \max_{\alpha, \beta} \{DP\}, \quad s.t. \quad (70)$$

$$C \geq C_m, \quad (71)$$

$$0 \leq \alpha \leq 1, \quad (72)$$

$$0 \leq \beta \leq 1 \quad (73)$$

where  $DP$  is given by (34) and  $C$  is given by (33), the second optimization problem is given by

$$P_8 : \max_{\alpha, \beta} \{C\}, \quad s.t. \quad (74)$$

$$DP \geq P_m, \quad (75)$$

$$0 \leq \alpha \leq 1, \quad (76)$$

$$0 \leq \beta \leq 1 \quad (77)$$

and the third optimization problem is given as

$$P_9 : \max_{\alpha, \beta} \{U\}, \quad s.t. \quad (78)$$

$$0 \leq \alpha \leq 1, \quad (79)$$

$$0 \leq \beta \leq 1. \quad (80)$$

In this scheme, the optimization is subject to constraints on both  $\alpha$  and  $\beta$  due to the mixture.

For  $P_7$  in (70), using (33) in (71), one has

$$(1-\beta)T \log_2(1+(1-\alpha)P_T\gamma_c) \geq C_m. \quad (81)$$

Using (81) and (72), one has

$$0 \leq \alpha \leq 1 + \frac{1}{P_T\gamma_c} - \frac{1}{P_T\gamma_c} 2^{\frac{C_m}{(1-\beta)T}} \quad (82)$$

$$0 \leq \beta \leq 1 - \frac{C_m}{T \log_2(1+P_T\gamma_c)} \quad (83)$$

where  $C_m < T \log_2(1+P_T\gamma_c)$  must be satisfied. One sees from (34) that  $DP$  is a monotonic function of  $\alpha$  so that the maximum  $P_D$  is achieved when  $\alpha$  is the largest, for any allowable values of  $\beta$ . Thus, from (82),  $DP$  is maximized when  $\alpha = 1 + \frac{1}{P_T\gamma_c} - \frac{1}{P_T\gamma_c} 2^{\frac{C_m}{(1-\beta)T}}$ . Using this relationship in (34),  $DP$  becomes a function of a single variable  $\beta$  as

$$DP = Q_1(\sqrt{2P_T\gamma_s N J}, b), \quad (84)$$

where  $J = \beta \left(1 + \frac{1}{P_T\gamma_c} - \frac{1}{P_T\gamma_c} 2^{\frac{C_m}{(1-\beta)T}}\right)$  and which is maximized when  $J$  is maximized, as the Marcum Q function is monotonic. By taking the first-order derivative of  $J$  with respect to  $\beta$  and setting the derivative to zero, one has the equation that determines the optimum  $\beta$  as

$$(1+P_T\gamma_c)2^{-\frac{C_m}{(1-\beta_{opt})T}} = 1 + \frac{C_m \log 2}{T} \frac{\beta_{opt}}{(1-\beta_{opt})^2} \quad (85)$$

where  $\beta$  satisfies (83). Once the optimum value of  $\beta$  is obtained from (85), the optimum values of  $\alpha$  and  $DP$  are derived as

$$\alpha_{opt} = 1 + \frac{1}{P_T\gamma_c} - \frac{1}{P_T\gamma_c} 2^{\frac{C_m}{(1-\beta_{opt})T}} \quad (86)$$

and

$$DP^{max} = Q_1(\sqrt{2\alpha_{opt}\beta_{opt}P_T\gamma_s N}, b) \quad (87)$$

respectively.

For  $P_8$  in (74), using (34) in (75), one has

$$Q_1(\sqrt{2\alpha\beta P_T\gamma_s N}, b) \geq P_m. \quad (88)$$

Since the Marcum Q function is monotonic, using (88) and (77), one has

$$1 \geq \beta \geq \frac{1}{\alpha} \frac{[Q_1^{-1}(P_m, b)]^2}{2P_T\gamma_s N} \quad (89)$$

$$1 \geq \alpha \geq \frac{[Q_1^{-1}(P_m, b)]^2}{2P_T\gamma_s N}. \quad (90)$$

From (33), the information rate  $R$  increases monotonically as  $\beta$  decreases. Thus, the maximum  $C$  is achieved when  $\beta$  is the smallest. From (89), this is given by  $\beta = \frac{1}{\alpha} \frac{[Q_1^{-1}(P_m, b)]^2}{2P_T\gamma_s N}$ . Using this relationship in (33), the rate becomes

$$C = \left(1 - \frac{1}{\alpha} \frac{[Q_1^{-1}(P_m, b)]^2}{2P_T\gamma_s N}\right) \cdot T \log_2(1+(1-\alpha)P_T\gamma_c) \quad (91)$$

which is a function of  $\alpha$  only. By taking the first-order derivative of  $C$  in (91) with respect to  $\alpha$  and setting the derivative to zero, one has

$$\begin{aligned} & \left(\frac{1}{P_T\gamma_c} + 1 - \alpha_{opt}\right) \log[1+(1-\alpha_{opt})P_T\gamma_c] \\ &= \frac{2P_T\gamma_s N}{[Q_1^{-1}(P_m, b)]^2} \alpha_{opt}^2 - \alpha_{opt} \end{aligned} \quad (92)$$



to find the optimum value of  $\alpha$  numerically, where  $\alpha$  satisfies (90). This equation cannot be solved in closed-form due to the logarithm function inside. Then, the optimum  $\beta$  and  $C$  are given by

$$\beta_{opt} = \frac{1}{\alpha_{opt}} \frac{[Q_1^{-1}(P_m, b)]^2}{2P_T\gamma_s N} \quad (93)$$

and

$$C^{max} = (1 - \beta_{opt})T \log_2(1 + (1 - \alpha_{opt})P_T\gamma_c) \quad (94)$$

respectively.

For  $P_9$  in (78), we can take the partial derivatives of  $U$  with respect to  $\alpha$  and  $\beta$  and setting them to zero to give

$$\begin{aligned} \epsilon \frac{\sqrt{\alpha P_T\gamma_s N}}{\sqrt{2\beta}} \frac{\partial Q_1(a', b)}{\partial a'} \\ = \frac{(1 - \epsilon) \log(1 + (1 - \alpha)P_T\gamma_c)}{\log(1 + P_T\gamma_c)} \end{aligned} \quad (95)$$

$$\begin{aligned} \epsilon \frac{\sqrt{\beta P_T\gamma_s N}}{\sqrt{2\alpha}} \frac{\partial Q_1(a', b)}{\partial a'} \\ = \frac{(1 - \epsilon)(1 - \beta)P_T\gamma_c}{(1 + (1 - \alpha)P_T\gamma_c) \log(1 + P_T\gamma_c)} \end{aligned} \quad (96)$$

where  $a' = \sqrt{2\alpha\beta P_T\gamma_s N}$ . Combining the above two equations, one has

$$\beta = \frac{\alpha P_T\gamma_c}{\alpha P_T\gamma_c + (1 + (1 - \alpha)P_T\gamma_c) \log(1 + (1 - \alpha)P_T\gamma_c)}. \quad (97)$$

Also, upon further simplification, one has

$$\begin{aligned} \frac{1 - \epsilon}{\epsilon \alpha_{opt} P_T\gamma_s N} \frac{\log(1 + (1 - \alpha_{opt})P_T\gamma_c)}{\log(1 + P_T\gamma_c)} \\ = Q_2\left(\sqrt{\frac{2\alpha_{opt} P_T\gamma_s N}{1 + \log(1 + (1 - \alpha_{opt})P_T\gamma_c)^c}}, b\right) \\ - Q_1\left(\sqrt{\frac{2\alpha_{opt} P_T\gamma_s N}{1 + \log(1 + (1 - \alpha_{opt})P_T\gamma_c)^c}}, b\right) \end{aligned} \quad (98)$$

which can be used to determine the optimum value for  $\alpha$ , where  $c = \frac{1}{\alpha_{opt} P_T\gamma_c} + \frac{(1 - \alpha_{opt})}{\alpha_{opt}}$ . Then, the optimum  $\beta$  and  $U$  are calculated as

$$\beta_{opt} = \frac{1}{1 + c \log(1 + (1 - \alpha_{opt})P_T\gamma_c)}. \quad (99)$$

and

$$\begin{aligned} U^{max} = \epsilon Q_1(\sqrt{2\alpha_{opt}\beta_{opt} P_T\gamma_s N}, b) \\ + (1 - \epsilon) \frac{(1 - \beta_{opt}) \log(1 + (1 - \alpha_{opt})P_T\gamma_c)}{\log(1 + P_T\gamma_c)}. \end{aligned} \quad (100)$$

In the next section, we will use numerical examples to show the effects of different system parameters on the performance tradeoff and optimization.

#### IV. NUMERICAL RESULTS AND DISCUSSION

In this section, numerical examples are presented to examine the performance of the considered joint radar-communications system. In the examination, we set  $C_m = 2$ ,  $P_m = 0.5$ ,  $\rho = 1$ ,  $\epsilon = 0.5$ ,  $FA = 0.01$ ,  $P_T = 1$  and  $T = 10$ , while we focus on the effects of  $\gamma_c$ ,  $\gamma_d$  and  $\gamma_s$  on the system performance.

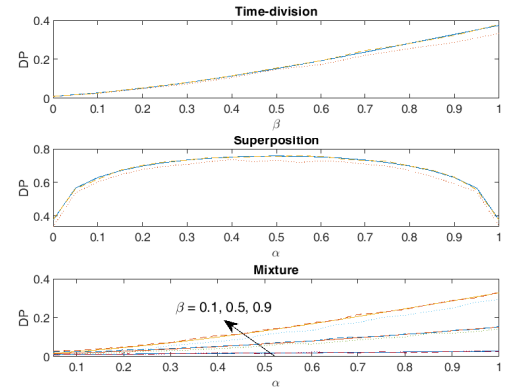


Fig. 2. Comparison of simulated (dashed line  $\gamma_d = 20dB$  and dotted line  $\gamma_d = 10dB$ ) and approximate (solid line)  $DP$  for time division, superposition and mixture schemes when  $\gamma_c = 10dB$  and  $\gamma_s = -5dB$ .

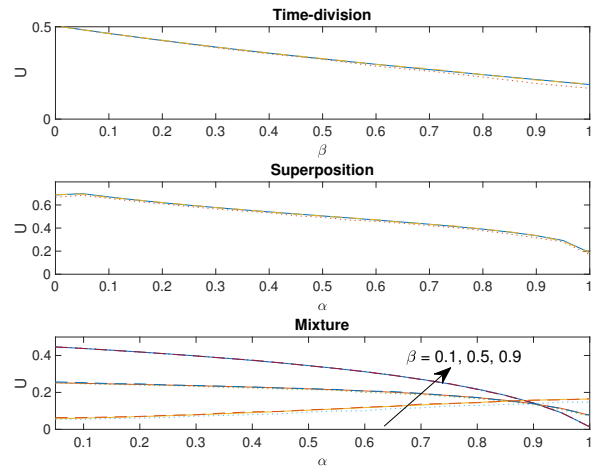


Fig. 3. Comparison of simulated (dashed line  $\gamma_d = 20dB$  and dotted line  $\gamma_d = 10dB$ ) and approximate (solid line)  $U$  for time division, superposition and mixture schemes when  $\gamma_c = 10dB$  and  $\gamma_s = -5dB$ .

The single-variable equations are solved by using the built-in function 'fminbnd' in MATLAB for all schemes to find the optimum values. The performance of communications is measured by the information rate  $C$ .

First, we examine the accuracies of the approximations in (9), (10), (19), (20), (27) and (28), as they are used for the derivations of the optimum values later on. To do this, we compare  $DP$  and  $U$  using the approximate results in (10), (20) and (28) with the detection threshold determined by (9), (19) and (28) with the simulated values using the detection threshold determined by (8) for  $\gamma_d = 20dB$  and  $\gamma_d = 10dB$ , respectively. Figs. 2 and 3 show the comparison of the time division, superposition and mixture schemes for  $DP$  and  $U$ , respectively. For the time division scheme, the approximation error in  $DP$  decreases when  $\beta$  decreases or  $\gamma_d$  increases. At  $\gamma_d = 20dB$ , the error can be ignored. For the superposition scheme, the approximation error in  $DP$  is large when  $\alpha$  is

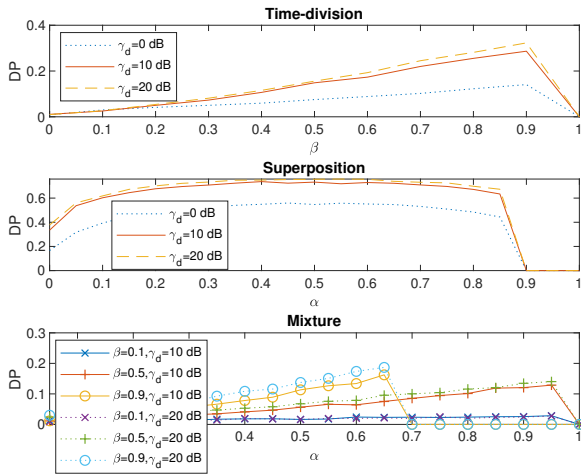


Fig. 4. The effect of  $\gamma_d$  on the simulated  $DP$  for the time division, superposition and mixture schemes when  $\gamma_c = 10$  dB and  $\gamma_s = -5$  dB.

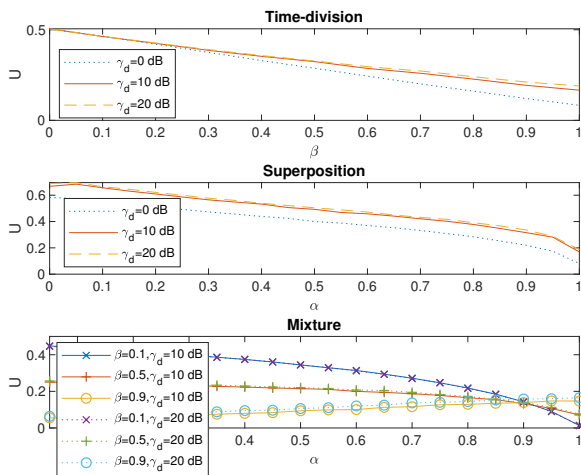


Fig. 5. The effect of  $\gamma_d$  on the simulated  $U$  for the time division, superposition and mixture schemes when  $\gamma_c = 10$  dB and  $\gamma_s = -5$  dB.

medium but is also negligible when  $\gamma_d$  is large. For the mixture scheme, the approximation error in  $DP$  is large when  $\beta$  is large or  $\alpha$  is medium, but otherwise is small. It also diminishes when  $\gamma_d$  increases from 10 dB to 20 dB. This agrees with the observation in [24]. For  $U$ , the approximation error is even smaller, as it is a weighted sum of  $DP$  and  $C$ . In most cases considered, the optimum values of  $\alpha$  and  $U$  from the approximate curves are almost the same as those from the simulated curves, implying that we can use the approximations to derive the optimum values.

Since the approximate expressions do not contain  $\gamma_d$ , we examine the effect of  $\gamma_d$  by simulation. Figs. 4 and 5 show the effect of  $\gamma_d$  on the optimization problems in (35) and (41), (55) and (61), (70) and (78) for the time-division, superposition and mixture schemes in terms of  $DP$  and  $U$ , respectively. One sees that both  $DP$  and  $U$  increase when  $\gamma_d$  increases, as expected, as a larger  $\gamma_d$  leads to be a stronger reference signal and hence

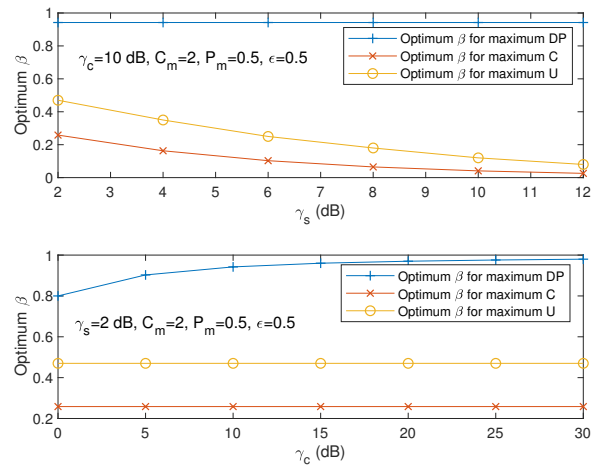


Fig. 6. The optimum value of  $\beta$  for different  $\gamma_c$  and  $\gamma_s$  in the time division scheme.

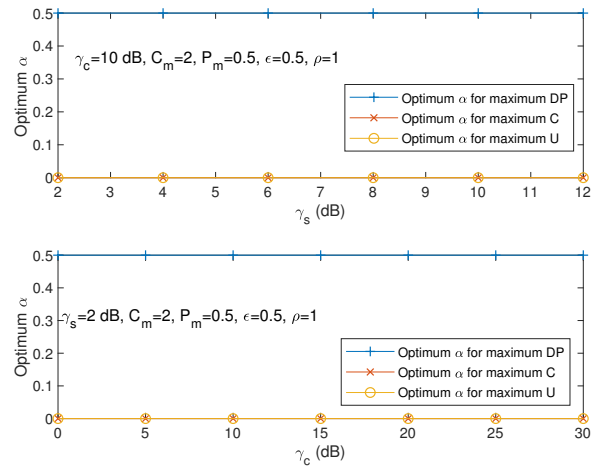


Fig. 7. The optimum value of  $\alpha$  for different  $\gamma_c$  and  $\gamma_s$  in the superposition scheme.

a better detection. One also notes that the optimum values of  $\alpha$  and  $\beta$  are almost identical for different values of  $\gamma_d$ . For example, in Fig. 4 for  $DP$ , the optimum  $\alpha$  is about 0.95 for  $\beta = 0.1$  and  $\beta = 0.5$ , and about 0.65 for  $\beta = 0.9$ , for all values of  $\gamma_d$ . In Figs. 4 and 5, the increase from  $\gamma_d = 10$  dB to  $\gamma_d = 20$  dB is much smaller than that from  $\gamma_d = 0$  dB to  $\gamma_d = 10$  dB. These figures imply that the effect of  $\gamma_d$  on the performance tradeoff is quite small.

Figs. 6 - 8 show how the optimum  $\alpha$  and  $\beta$  change for different values of  $\gamma_c$  and  $\gamma_s$  in the time-division, superposition and mixture schemes, respectively. From Fig. 6, the optimum  $\beta$  decreases with  $\gamma_s$  for the optimization problems in  $P_2$  and  $P_3$  and stays approximately the same for  $P_1$ . Also, the optimum  $\beta$  changes little with  $\gamma_c$ . Also, from Fig. 7, the optimum  $\alpha$  stays constant at 0.5 for the optimization problem in  $P_4$  and 0 for  $P_5$  and  $P_6$ . This is because our choices of parameters satisfy the first conditions in (64) and (67). From Fig. 8, when  $\gamma_c$  increases, the optimum values of  $\alpha$  and  $\beta$  in  $P_7$  increase. When  $\gamma_c$  increases, the communications channel becomes better so that the information rate increases. As such, to satisfy a fixed

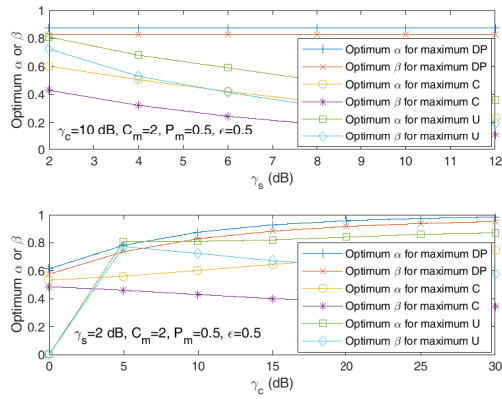


Fig. 8. The optimum values of  $\alpha$  and  $\beta$  for different  $\gamma_c$  and  $\gamma_s$  in the mixture scheme.

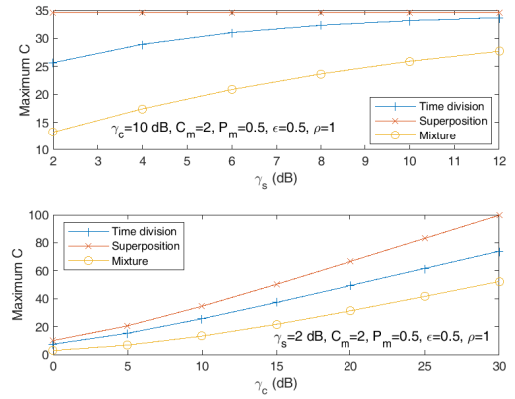


Fig. 10. Comparison of the maximized  $C$  for the time division, superposition and mixture schemes.

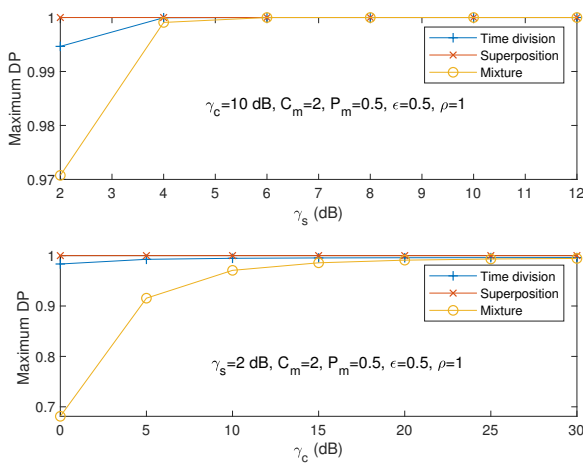


Fig. 9. Comparison of the maximized  $DP$  for the time division, superposition and mixture schemes.

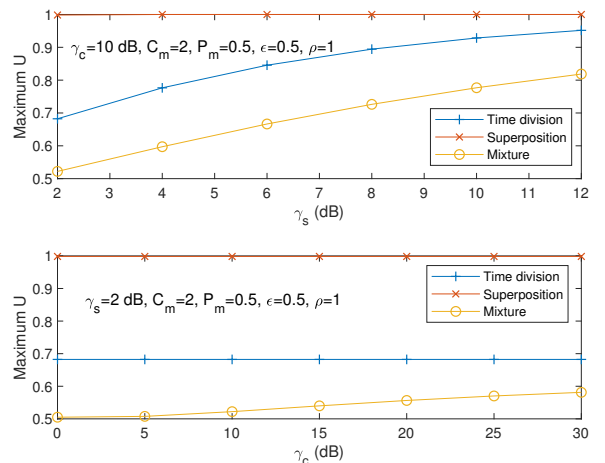


Fig. 11. Comparison of the maximized  $U$  for the time division, superposition and mixture schemes.

minimum rate, more time and more power can be allocated to the radar signal for higher probability of detection. This leads to the increase of  $\alpha$  and  $\beta$ . Also, when  $\gamma_c$  increases, the optimum  $\alpha$  increases while the optimum  $\beta$  decreases in  $P_8$ . Since  $P_8$  requires a fixed minimum probability of detection, from (34),  $\alpha\beta$  must be fixed so that either  $\alpha$  increases and  $\beta$  decreases or  $\alpha$  decreases and  $\beta$  increases. From (33),  $C$  has a linear relationship with  $\beta$  and a logarithmic relationship with  $\alpha$ . Thus, to maximize  $C$ , a decrease of  $\beta$  and an increase of  $\alpha$  work better, as in Fig. 8. For  $P_9$ , when  $\gamma_s$  increases, the optimum  $\alpha$  and  $\beta$  decrease and when  $\gamma_c$  increases, the optimum  $\alpha$  and  $\beta$  first increase then decrease. In most cases,  $\gamma_c$  and  $\gamma_s$  have significant impact on the optimization.

Figs. 9 - 11 compare the maximum  $DP$ ,  $C$  and  $U$ , respectively, using the optimum values of  $\alpha$  and  $\beta$  in Figs. 6 - 8. of the time-division scheme and those of the superposition scheme for different values of  $\gamma_c$  and  $\gamma_d$ . It can be seen that the maximum values either increase or stay the same, as  $\gamma_c$  and  $\gamma_s$  increase, as expected, as better channel conditions lead to better performances. It can also be seen that the superposition scheme outperforms the time division and mixture schemes

with considerable performance gains in all the cases considered. For example, the maximum  $DP$  of the superposition scheme is almost fixed at 1 for all values of  $\gamma_c$  and  $\gamma_s$  considered in Fig. 9, while the maximum  $DP$  of the time-division and mixture schemes only reaches 1 for large values of  $\gamma_c$  and  $\gamma_s$ . This can be explained as follows. From (7), (17) and (25), the amplitude of the sample in the superposition scheme is larger than those in the time-division and mixture schemes. Since both the communications signal and the radar signal are assumed deterministic and unknown, more signal energy can be captured in the GLRT detection using the superposition scheme for better detection performances. Also, since the superposition scheme uses the whole time period of  $T$  seconds for communications, its information rate is higher than the time-division and mixture schemes that only uses  $T_c$  seconds for communications but with a higher SNR, as the information rate has a linear relationship with the time and a logarithmic relationship with the SNR. On the other hand, the large amplitude of the superposition scheme also leads to a higher peak-to-average-power ratio for the transmitted signal, which may not be desirable in some systems.

It is noted that both the superposition and time division schemes use a total energy of  $P_T T$ , while the mixture scheme only uses a total energy of  $P_c T_c + P_r T_c$ . Hence, the mixture scheme uses a smaller total energy. In this sense, the comparison in Figs. 9 - 11 may not be fair for the mixture scheme. However, the comparison shows that, in some cases, such as  $DP$  in Fig. 9 when  $\gamma_s > 4dB$  and  $\gamma_c > 15dB$ , the mixture scheme is as good as the time division and superposition schemes that require more energy. Thus, the mixture scheme is an energy-efficient scheme in these cases, and the comparison is useful. Note also that the dual-functional waveform method achieves radar-communications tradeoff by adjusting the transmitted pulse while our method, including [20] - [24], does this by adjusting the transmission power and time. Thus, they are two different categories of methods with different complexities and are not compared here.

## V. CONCLUSION

In this paper, three schemes of joint radar-communications designs have been studied by using time division, superposition or their mixture. For each scheme, three optimization problems have been formulated and solved. Numerical results have shown that the superposition scheme is better than the time division and mixture schemes and that the SNRs in the surveillance channel and the communications channel have more significant impact on the tradeoff and the optimization than the SNR in the direct channel. Future works will consider other types of radar and use other detection methods for radar. This includes multiple-input-multiple-output (MIMO) radar as well as MIMO communications. Other multiplexing methods will be considered, such as orthogonal frequency division multiplexing and code division multiple access. It is also interesting to apply the analysis to a specific scenario for practical verification. Finally, the system considered assumes a single receiving vehicle and a single obstacle. The proposed designs can be extended to multiple vehicles and multiple obstacles moving in an urban area to sense the driving environment using radar.

## REFERENCES

- [1] B. Paul, A.R. Chiriyath, D.W. Bliss, "Survey of RF communications and sensing convergence research," *IEEE Access*, vol. 5, pp. 252 - 270, 2017.
- [2] R. Bishop, *Intelligent Vehicle Technology and Trends*, Norwood, MA: Artech House, 2005.
- [3] P. Kumari, J. Choi, N. Gonzalez-Prelcic, and R. W. Heath, "IEEE 802.11ad-based radar: an approach to joint vehicular communication-radar system," *IEEE Transactions on Vehicular Technology*, vol. 67, pp. 30123027, April 2018.
- [4] S.H. Dokhanchi, M.R.B. Shankar, T. Stifter, B. Ottersten, "OFDM-based automotive joint radar-communication system," *Proc. IEEE Radar Conference*, Oklahoma, USA, April 2018.
- [5] S.H. Dokhanchi, B.S. Mysore, K.V. Mishra, B. Ottersten, "A mmWave automotive joint radar-communications system," *IEEE Trans. Aerospace and Electronic Sys.*, vol. 55, pp. 1241 - 1260, June 2019.
- [6] G. Soatti, M. Nicoli, N. Garcia, B. Denis, R. Raulefs, H. Wymeersch, "Enhanced vehicle positioning in cooperative ITS by joint sensing of passive features," *Proc. IEEE Int. Conf. Intelligent Transportation Systems*, Yokohama, Japan, Oct. 2017.
- [7] E. Strom, H. Hartenstein, P. Santi, W. Wiesbeck, "Vehicular communications: Ubiquitous networks for sustainable mobility," *Proc. IEEE*, vol. 98, no. 7, pp. 1111-1112, Jul. 2010.
- [8] M. Ghorbanzadeh, E. Vistosky, P. Moorut, W. Yang, C. Clancy, "Radar in-band interference effects on macrocell LTE uplink deployments in the US 3.5 GHz band," *Proc. 2015 IEEE International Conference on Computing, Networking and Communications*, pp. 248 - 254, Garden Grove, USA, 2015.
- [9] M.P. Masarik, N.S. Subotic, "Cramer-Rao lower bounds for radar parameter estimation in noise plus structured interference," *Proc. IEEE Radar Conference*, pp. 1-4, Philadelphia, USA, May 2016.
- [10] T. Tian, T. Zhang, L. Kong, G. Cui, Y. Wang, "Mutual information based partial band coexistence for joint radar and communication system," *Proc. IEEE Radar Conf.*, Boston, USA, April 2019.
- [11] F. Liu, C. Masouros, A. Li, T. Ratnarajah, J. Zhou, "MIMO radar and cellular coexistence: a power-efficient approach enabled by interference exploitation," *IEEE Trans. Signal Processing*, vol. 66, pp. 3681 - 3695, July 2018.
- [12] E. Grossi, M. Lops, L. Venturino, "Joint design of surveillance radar and MIMO communication in cluttered environments," *IEEE Trans. Signal Processing*, Feb. 2020.
- [13] Z.-M. Jiang, P.-C. Zhang, L. Huang, X. He, J.-H. Zhang and M. Rihan, "Transmit beampattern optimization for automotive MIMO radar coexisted with communication in V2V networks," *Sensors*, vol. 20, 2020.
- [14] S. Sodagari, A. Khawar, T.C. Clancy, R. McGwier, "A project based approach for radar and telecommunication systems coexistence," *Proc. Globecom 2012*, pp. 1-5, Anaheim, USA, Dec. 2012.
- [15] C. Sturm and W. Wiesbeck, "Waveform design and signal processing aspects for fusion of wireless communications and radar sensing," *Proc. IEEE*, vol. 99, pp. 1236 - 1259, July 2011.
- [16] C.S. Pappu, T.L. Carroll, B.C. Flores, "Simultaneous radar-communication systems using controlled chaos-based frequency modulated waveforms," *IEEE Access*, vol. 8, pp. 48361 - 48375, Mar. 2020.
- [17] S. Shi, Z. Wang, Z. He, Z. Cheng, "Constrained waveform design for dual-functional MIMO radar-communication system," *Signal Processing*, vol. 171, June 2020.
- [18] Y. Yao, P. Miao, Z. Chen, "Cognitive waveform optimization for phase-modulation-based joint radar-communications system," *IEEE Access*, vol. 8, pp. 33276 - 33288, Feb. 2020.
- [19] K.V. Mishra, M.R.B. Shankar, V. Koivunen, B. Ottersten, S.A. Vorobyov, "Toward millimeter-wave joint radar communications: a signal processing perspective," *IEEE Signal Processing Mag.*, vol. 36, pp. 100 - 114, Sept. 2019.
- [20] G. Cui, J. Liu, H. Li, B. Himed, "Signal detection with noisy reference for passive sensing," *Signal Processing*, no. 108, pp. 389 - 399, 2015.
- [21] Y. Chen, Y. Wu, N. Chen, W. Feng, J. Zhang, "New approximate distributions for the generalized likelihood ratio test detection in passive radar," *IEEE Signal Processing Letters*, vol. 26, pp. 685 - 689, May 2019.
- [22] D.E. Hack, L.K. Patton, B. Himed, M.A. Saville, "Detection in passive MIMO radar networks," *IEEE Trans. Signal Processing*, vol. 62, pp. 2999 - 3012, June 2014.
- [23] D.E. Hack, L.K. Patton, B. Himed, M.A. Saville, "Centralized passive MIMO radar detection without direct-path references," *IEEE Trans. Signal Processing*, vol. 62, pp. 3013 - 3023, June 2014.
- [24] B.K. Chalise, M.G. Amin, B. Himed, "Performance tradeoff in a unified passive radar and communications system," *IEEE Signal Processing Letters*, vol. 24, pp. 1275 - 1279, Sept. 2017.
- [25] J. Li, P. Stoica, *MIMO Radar Signal Processing*, John Wiley & Sons: Hoboken, NJ, 2009.
- [26] X. Wang, A. Hassanien, M.G. Amin, "Dual-function MIMO radar communications system design via sparse array optimization," *IEEE Trans. Aerospace and Electronic Systems*, vol. 55, pp. 1213 - 1226, June 2019.
- [27] T. Brenner, G. Weiss, M. Klein, H. Kuschel, "Signals and data fusion in a deployable multiband passive-active radar (DMPAR)," *IET Int. Conf. on Radar Systems*, Glasgow, UK, Oct. 2012.
- [28] A.R. Chiriyath, B. Paul, and D.W. Bliss, "Radar-Communications Convergence: Coexistence, Cooperation, and Co-Design," *IEEE Transactions on Cognitive Communications and Networking*, vol. 3, pp. 112, March 2017.
- [29] Y. Chen, Y. Wu, J. Zhang, N. Chen, "New estimators for primary channel gain in cognitive radio networks," *IEEE Communications Letters*, vol. 22, pp. 2435 - 2438, Dec. 2018.
- [30] D. Poullin, "Passive detection using digital broadcasters (DAB, DVB) with COFDM modulation" *Proc. IEE*, vol. 152, pp. 143 - 152, June 2005.
- [31] R.S.A.R. Abdullah, A.A. Salah, A. Ismail, F.H. Hashim, N.E.A. Rashid, N.H.A. Aziz, "Experimental investigation on target detection and track-

- ing in passive radar using long-term evolution signal," *IEE-Radar, Sonar & Navigation*, vol. 10, pp. 577 - 585, Feb. 2016.
- [32] I.S. Gradshteyn and I.M Ryzhik, *Table of Integrals, Series and Products*, 7th Ed. Academic Press: London, UK. 2007.